JOC The Journal of Organic Chemistry

Article

pubs.acs.org/joc

1-, 3-, 6-, and 8-Tetrasubstituted Asymmetric Pyrene Derivatives with Electron Donors and Acceptors: High Photostability and Regioisomer-Specific Photophysical Properties

Yosuke Niko,*[,†] Shunsuke Sasaki,[†] Kaishi Narushima,[†] Dharmendar Kumar Sharma,[†] Martin Vacha,[†] and Gen-ichi Konishi*[,†,‡]

[†]Department of Organic and Polymeric Materials, Tokyo Institute of Technology, 2-12-1-H-134 O-okayama, Meguro-ku, Tokyo 152-8552, Japan

[‡]PRESTO Japan Science and Technology Agency, Tokyo 102-0076, Japan

Supporting Information

ABSTRACT: The systematic synthesis of five 1-, 3-, 6-, and 8-tetrasubstituted asymmetric pyrenes with electron donor and acceptor moieties is presented, together with an examination of their photophysical properties. Pyrene derivative **PA1**, containing one formyl and three piperidyl groups, showed bright solvatochromic fluorescence from green (λ_{em} = 557 nm, Φ_{FL} = 0.94 in hexane) to red (λ_{em} = 648 nm, Φ_{FL} = 0.50 in methanol), suggesting potential applications for **PA1** as an environmentally responsive probe. Although the synthesis of simple 1- and 3-disubstituted pyrene derivatives is considered difficult, **PA13**, with two formyl groups at the 1- and 3-positions and two piperidyl groups at the 6- and 8-positions, could be synthesized successfully. **PA13** exhibited less pronounced solvatochromism, but displayed a narrow fluorescent band with high Φ_{FL} in all solvents (Φ_{FL} > 0.75). Moreover, its absorption band displayed an exceptional bathochromic shift compared to the other derivatives (e.g., λ_{abs} = 480 and 522 nm in ethanol for **PA1** and **PA13**, respectively), suggesting that such modifications of pyrene may be quite important for the modulation of its energy gap. Additionally, all compounds exhibited exceptionally high photostability, which highlights the advantage of these new dyes and provides new insights on the design of photostable fluorophores.

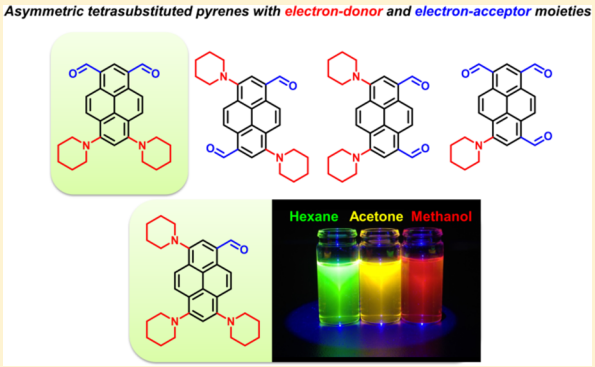

INTRODUCTION

Over the past decades, the polycyclic aromatic hydrocarbon (PAH) pyrene has been essential in the development of various materials. Initially, pyrene received attention due to its specific fluorescence characteristics such as the Ham effect[1] and the excimer emission,[2] which are triggered by changes of the environmental polarity and changes of the local pyrene concentration, respectively. Therefore, pyrene and its analogues have traditionally been widely used as fluorescence probes, capable of providing information regarding the local polarity, as well as on the dynamics of specific small compounds and macromolecules, especially in the area of biomedicine and soft materials.[3] Furthermore, because a variety of pyrene derivatives exhibit an intense blue emission, outstanding chemical stability, high charge carrier mobility, and hole injection ability, they have attracted considerable attention as semiconductors[4] for applications in organic electronics such as organic light-emitting diodes,[5] organic field-effect transistors,[6] and organic photovoltaic devices.[7] Most recently, pyrene has been used as a building block for the construction of metal−organic frames or covalent organic frame materials,[8] structurally uniform nanocarbon materials,[9] and discotic liquid crystals.[10] Moreover, pyrene-based chemosensors and photodynamic therapy materials have been further advanced.[11]

One of the main reasons why pyrene is used so frequently in such diverse scientific fields is the facile control over the structural and electronic properties of pyrene by chemical manipulations. Therefore, continuous efforts are directed toward an expansion of the available derivatization methodologies for pyrene (Figure 1a).[12−16] Although pyrene is usually modified by mono-, di-, or tetra-substitution at its 1-, 3-, 6-, and 8-positions,[4] Yamato[12a] and Müllen[12b] demonstrated that the introduction of a tertiary alkyl group at the 7-position as a potential protective group enables the selective modification of the 1- and 3-positions. Similarly, they also succeeded in modifying the 4-, 5-, 9-, and 10-positions (K region).[6a,13] Moreover, Marder et al. reported an efficient modification at the 2- and/or 7-position by using an iridium catalyst.[5e,14] Such continuous progress has undoubtedly contributed to the popularity of pyrene as a building block in materials science.

Received: August 25, 2015
Published: October 15, 2015

DOI: 10.1021/acs.joc.5b01987
J. Org. Chem. 2015, 80, 10794−10805

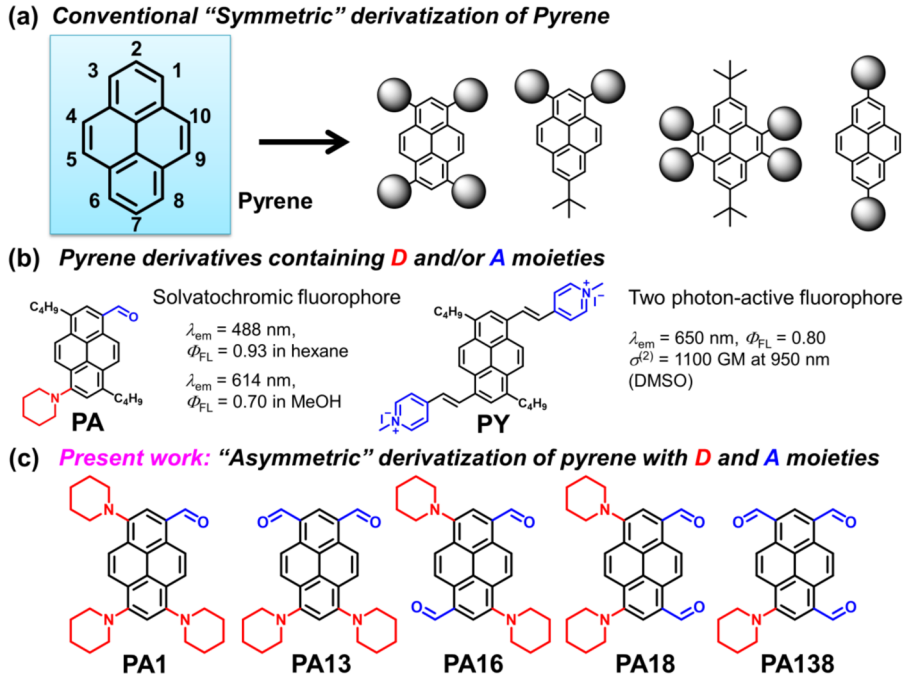

Figure 1. Schematic outline of (a) classical "symmetric" pyrene derivatives, (b) simple D- and/or A-substituted pyrene derivatives, and (c) "asymmetric" 1-, 3-, 6- and 8-tetrasubstituted pyrene derivatives targeted in this work.

However, almost all multisubstituted pyrene derivatives developed to date have been synthesized in a "symmetric" manner, i.e., the modification have been carried out using identical substituents. Despite the important role π-systems with D/A moieties play in a variety of applications, such as, e.g., long wavelength-absorbing dyes, two photon-absorbing dyes, and environmentally responsive dyes,[15] the number of asymmetric pyrene derivatives, in particular those containing electron donor (D) and/or electron acceptor (A) moieties, are extremely scarce except for a few examples.[16,17] This situation should most likely be attributed to two reasons: (1) for most chemists, pyrene is synonymous with the aforementioned Ham effect and excimer emission; i.e., they think of pyrene in terms of blue emission and usually do not consider D/A modifications; (2) the multitude of substitution sites available in pyrene allows a high number of D/A structures to be envisioned (including isomers), which may render the systematic synthesis of pyrene-based D/A derivatives complicate.

Nevertheless, our groups recently demonstrated that simple pyrene derivatives containing D and/or A moieties exhibit unique photophysical properties (Figure 1b).[19,20] For example, D−π−A-shaped pyrene **PA**,[19] which contains formyl (A) and piperidyl (D) groups at its 1- and 6-positions, respectively, showed bright and strong solvatochromic fluorescence in apolar and polar solvents. This phenomenon is due to the presence of a stable first singlet π−π^* excited state ($S_1(\pi-\pi^*)$) and a moderate change of the dipole moment between the ground and excited state ($\Delta\mu$) of **PA**.[19] Moreover, A−π−A-type pyrene **PY**, which contains vinyl-linked pyridinium iodide (A) at its 1- and 6-positions, exhibited a large two-photon absorption cross section and intense fluorescence in the spectral window used for the examination of biological tissue (650−1100 nm).[20] As these outstanding properties are unique to pyrene and arise from its inherent electronic and/or structural properties, further investigations regarding diverse pyrene D/A derivatives should be justified. It should be easily possible to tune the electronic properties of aromatic compounds containing D/A moieties by changing the nature, number, and substitution site of these moieties.[18] Simultaneously, such investigations should also be helpful to overcome the aforementioned synthetic problems associated with pyrene, which would be desirable from a general synthetic perspective.

This paper presents the development of a systematic and efficient synthesis of five asymmetric 1-, 3-, 6-, and 8-tetrasubstituted pyrene-based D/A derivatives (Figure 1c). To the best of our knowledge, the synthesis of such derivatives has not been achieved before. In particular, the synthetic procedure for **PA13**, which contains two formyl groups at the 1- and 3-positions as well as two piperidyl groups at the 6- and 8-positions, was expected to be challenging because even a simple modification of the 1- and 3-positions without protecting the 7-position is nontrivial. Subsequently, we characterized the regioisomer-specific photophysical properties of these tetrasubstituted pyrenes, as these are representative for their electronic properties and should thus facilitate an understanding of the underlying structure−property relationships. We observed that **PA1** showed the strongest and brightest solvatochromic fluorescence from green to red. Remarkably, **PA1** exhibited a much higher photostability relative to the commonly used solvatochromic fluorescent probe Nile Red (**NR**)[21] as well as to the other derivatives used in this study, thus highlighting its potential as a fluorescent probe. Moreover, **PA13** showed other exceptional optical behavior, i.e., a substantial bathochromically shifted absorption together with a strong and narrow, but less solvatochromic fluorescence, suggesting that the substitution pattern in this molecule is important for the modulation of the molecular band gap. Considering that all of the obtained pyrenes can be further derivatized, this study is expected to provide access to new research avenues to pyrene as a synthetic building block for advanced optoelectronic materials.

DOI: 10.1021/acs.joc.5b01987
J. Org. Chem. 2015, 80, 10794−10805

Scheme 1. Synthesis of PA1 and PA138

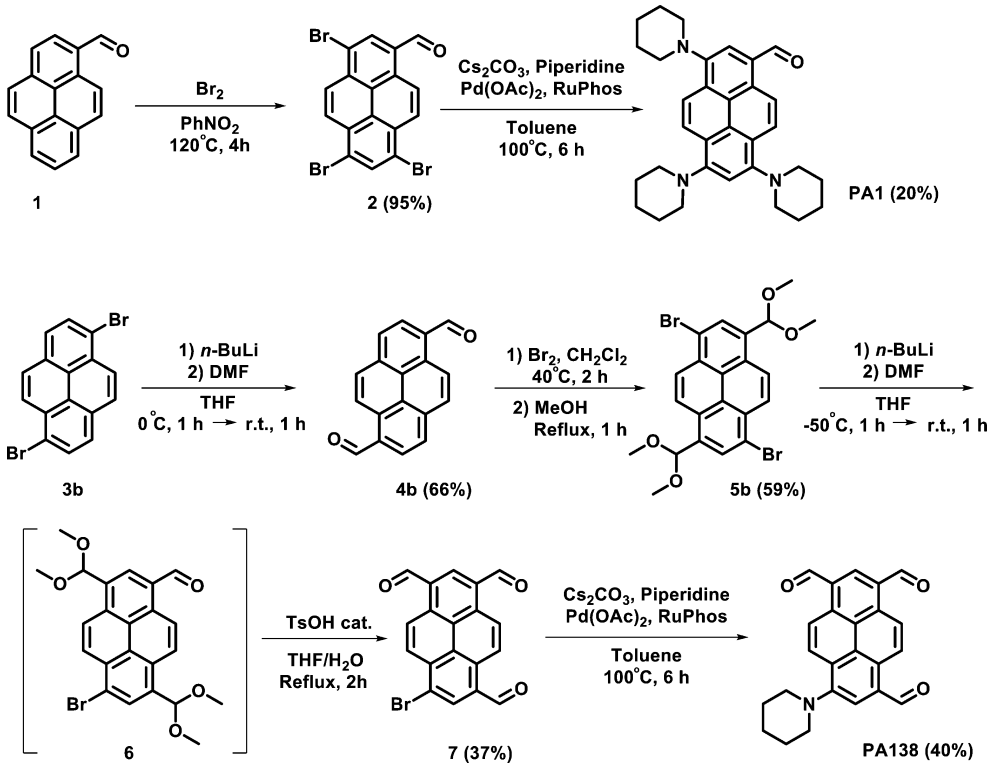

Scheme 2. Synthetic Route to 1,3-, 1,6-, and 1,8-Diformylpyrenes 4a−c

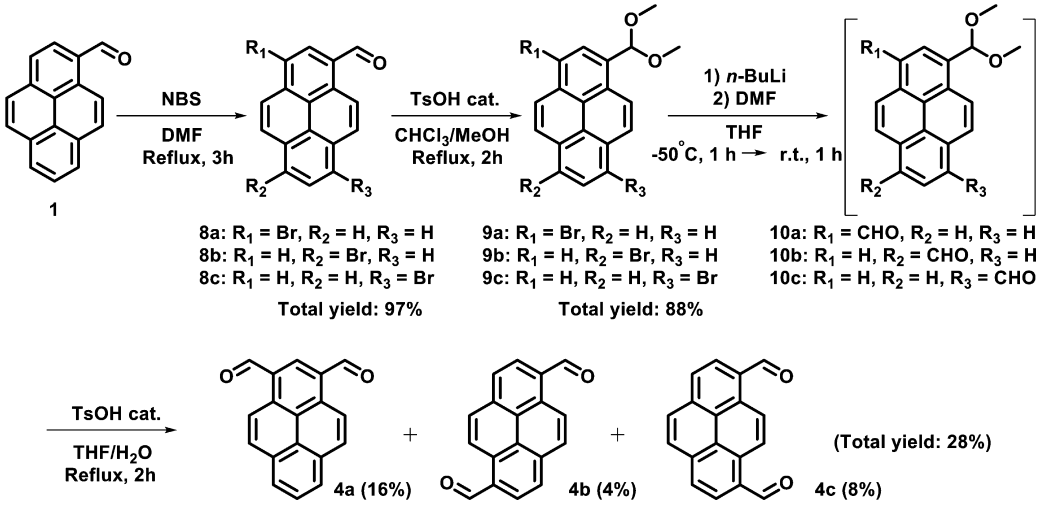

RESULTS AND DISCUSSION

Molecular Design and Synthetic Strategies. Initially we aimed at the development of suitable synthetic routes for the targeted pyrene-based D/A derivatives **PA1**, **PA13**, **PA16**, **PA18**, and **PA138** (Figure 1c), which are labeled according to the number and positions at which the formyl groups are attached on the pyrene ring. Piperidine and formyl groups were selected as substituents, as they have an established track record as D and A groups, respectively.[18] Additionally, the presence of formyl groups should be useful for future derivatization purposes, as they can be easily modified, using several well-established methods such as the Knoevenagel condensation[20] and the Wittig reaction, or converted into other functional groups such as carboxylic acid, ester, ketone, alcohol, or halide moieties.

All compounds were prepared in a uniform manner; i.e., the intermediates possessing the aldehyde and bromide substituents corresponding to the target compounds were synthesized initially to ensure that the 1-, 3-, 6-, or 8-positions were correctly substituted. Subsequently, the piperidine substituents were introduced by a Buchwald−Hartwig amination.[22]

Synthesis of PA1 and PA138. The synthetic routes to **PA1** and **PA138** are shown in Scheme 1. **PA1** contains one formyl group at the 1-position and three piperidyl groups at the 3, 6, and 8-positions. Similarly, **PA138** contains three formyl groups at the 1-, 3-, and 8-positions and one piperidyl group at the 6-position. Following the method reported by Korshun et al.,[23]

DOI: 10.1021/acs.joc.5b01987
J. Org. Chem. 2015, 80, 10794−10805

Scheme 3. Synthetic Route to PA13 and PA16

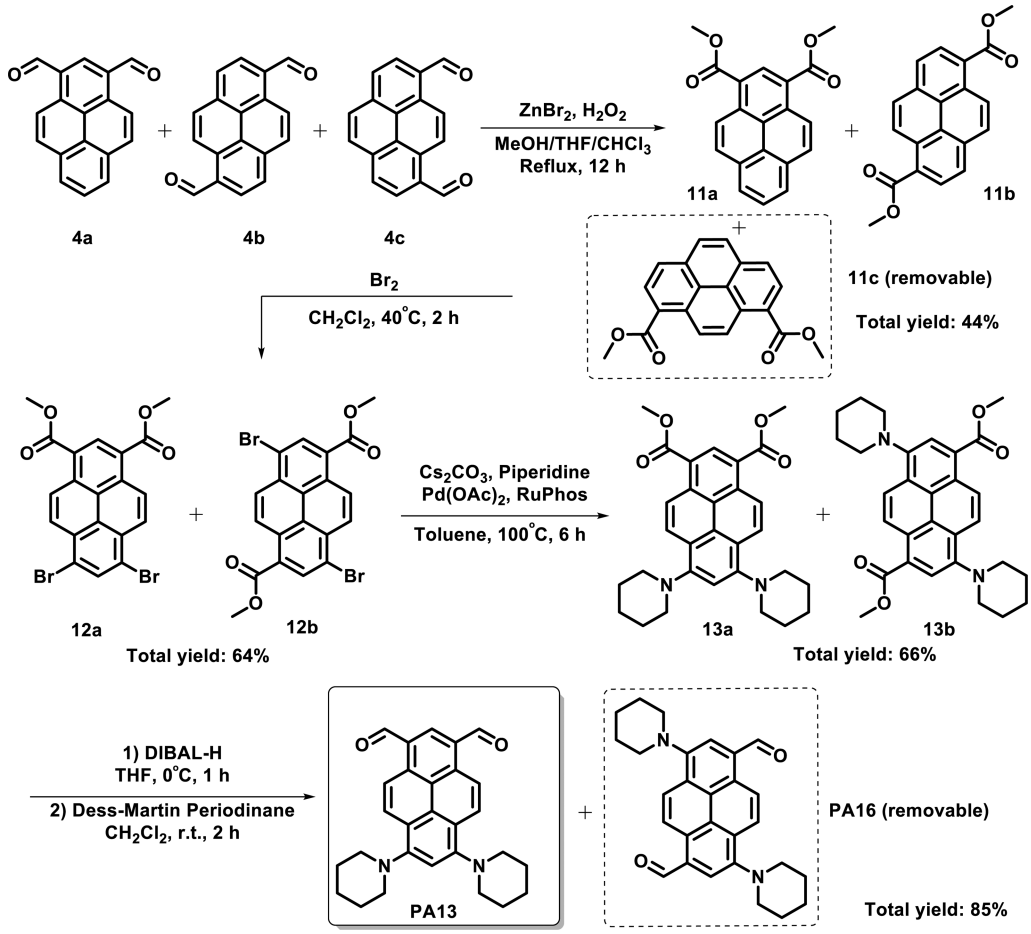

PA1 was synthesized in only two steps: the first involved the tribromination of 1-formylpyrene, followed by a Buchwald–Hartwig amination with piperidine. The yield of this amination was relatively low (20%), possibly because intermediate **2** contained some impurities. In fact, the presence of more than two bromide substituents drastically reduced the solubility of 1-formylpyrene in most suitable solvents, thus complicating the purification and detailed characterization of **2**. **PA138** was synthesized starting from 1,6-dibromopyrene **3b**, which was dilithiated with *n*-BuLi and subsequently treated with DMF to form 1,6-diformylpyrene (**4b**). This compound was subjected to a one-pot dibromination and concomitant protection of the two formyl groups as dimethyl acetals. The resulting derivative **5b** was lithiated using one equivalent of *n*-BuLi, before being treated with DMF to afford **6**, which was subsequently deprotected to recover the less soluble intermediate **7** by filtration. Target compound **PA138** was obtained after a final Buchwald–Hartwig amination.

Synthesis of PA13, PA16, and PA18. The synthetic routes to **PA13**, **PA16**, and **PA18** are outlined in Schemes 2–5. Each compound contains two formyl and two piperidyl groups, which differ in their arrangement with respect to each other on the pyrene ring. **PA16** and **PA18** were efficiently prepared in a manner similar to **PA138**, as 1,6- and 1,8-diformylpyrene were obtained from the corresponding dibromopyrene, which is available both synthetically and commercially (Scheme 4 and 5). However, this is certainly not the case for **PA13**, as an efficient synthesis of 1,3-dibromopyrene has not be achieved so

Scheme 4. Large-Scale Synthesis of 1,6-, and 1,8-Diformylpyrenes

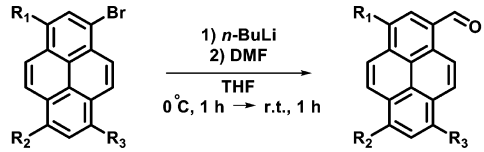

3b: R_1 = H, R_2 = Br, R_3 = H
3c: R_1 = H, R_2 = H, R_3 = Br

4b: R_1 = H, R_2 = CHO, R_3 = H (66%)
4c: R_1 = H, R_2 = H, R_3 = CHO (55%)

far without using a tertiary alkyl group at the 7-position as a protective group. Although the efficient synthesis of 1,3-diformylpyrene has been the focus of some research effort,[24] a simple yet effective method remains elusive so far. However, some reports have indicated the possibility of accessing 1,3-disubstituted pyrenes as follows: Korshun[23] and Tsubota[25] demonstrated a bromination at the 3-position in 1-acetylpyrene; i.e., they showed that the presence of an electron-withdrawing group at the 1-position enables electrophilic substitution at the 3-position. Similarly, Harvey[26] and Scott[27] demonstrated that a Friedel–Crafts acylation provides access to 1,3-diacetylpyrene, where the first acetyl group should function as an electron-withdrawing group. Encouraged by these reports, we initially tested a corresponding Friedel–Crafts formylation. However, the desired formylation could not be observed, which is probably due to the stronger electron-withdrawing property of the formyl group relative to the acetyl group. Therefore, we

DOI: 10.1021/acs.joc.5b01987
J. Org. Chem. 2015, 80, 10794–10805

Scheme 5. Large-Scale Synthesis of PA16 and PA18

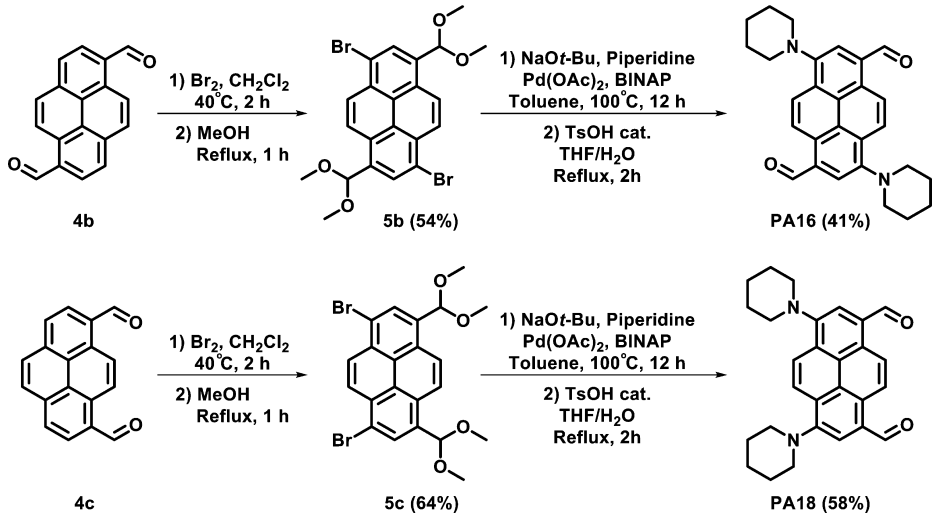

followed the method of Korshun and Tsubota, and used a bromination of 1-formylpyrene (Scheme 2).

The bromination of 1-formylpyrene afforded three isomers (**8a**–**c**), which were protected as dimethyl acetals (**9a**–**c**), before the bromide moieties were converted into formyl groups by lithiation with *n*-BuLi and treatment with DMF. The thus obtained compounds (**10a**–**c**) were deprotected to produce three diformylpyrene isomers (**4a**–**c**). Small amounts of each isomer could be separated by column chromatography on silica gel, followed by a subsequent fractional recrystallization from chloroform, and allowed their characterization by ^{1}H NMR spectroscopy (Figure S5). Nevertheless, the separation of these isomers at this stage proved to be impractical, because their R_f values were too similar and the compounds showed similar crystallization behavior. Therefore, the next reaction was carried out without further separation (Scheme 3). The formyl groups of **4a**–**c** were converted to methylester groups using the zinc-catalyzed oxidative esterification developed by Wu.[28] It is noteworthy to consider two important aspects of this process here. First, this esterification facilitated the removal of **11c** by column chromatography on silica gel, which is an absolutely critical procedure, as **PA13** cannot be separated from **PA18** by column chromatography on silica gel in the last step. Second, unlike **4b** and **4c**, **4a** could not be dibrominated efficiently in the next step without esterification (Scheme 5), which is probably due to the reduced solubility of monobrominated **4a**. After the introduction of the piperidyl groups by Buchwald–Hartwig amination, the ester groups of **12a**–**b** were initially reduced to the corresponding methyl alcohol groups using diisobutylaluminum hydride (DIBAL-H), before being subsequently converted to formyl groups under Dess–Martin oxidation conditions. The thus obtained isomers **PA13** and **PA16** could be easily separated by column chromatography on silica gel. It should be noted that not only **PA13**, but also **PA16** and even **PA18** can be prepared simultaneously in the same manner.

All the final products are soluble in common organic solvents, and were characterized by high-resolution mass spectroscopy as well as ^{1}H and ^{13}C NMR spectroscopy (see Supporting Information). Except for **PA1**, none of the compounds showed a clear melting point before decomposing.

As previously mentioned, the synthetically asymmetric 1-, 3-, 6-, 8-tetrasubstituted pyrene derivatives presented herein have not been synthesized before. In particular, the achievement of a successful synthetic route to **PA13** should be considered as an important breakthrough, because already the synthesis of a 1,3-disubstituted pyrene was considered particularly challenging. The synthetic routes described here might seem complicated and inefficient, but each reaction step proceeds quite rapidly and does not require complicated procedures. Therefore, we believe that these schemes deserve merit for their practicality. Considering that several other transition metal-catalyzed reactions should be applicable, and that the formyl groups could be easily converted to other functional groups, our synthetic methodology should represent a new milestone for researchers who want to use functionalized pyrene as a building block for advanced materials.

Photophysical Properties. As an example for structure–property relationships, we investigated the photophysical properties of the new pyrene derivatives in organic solvents of different polarity and compared them to those of **NR**, which is a commonly used solvatochromic fluorophore. In addition, the photostability of the new dyes was examined, because this property often presents a crucial bottleneck for commercial applications of solvatochromic fluorophores.[18d] Furthermore, we performed DFT/TD-DFT calculations on these pyrene dyes in order to gain a better understanding of their photophysical behavior.

Overview. The absorption and fluorescence spectra, as well as other spectroscopic properties and the results of quantum-chemical calculations for **PA1**, **PA18**, **P16**, **PA13**, and **PA138** are summarized in the Supporting Information. In general, all compounds showed maximum absorption peaks in the visible region with absorption coefficients of approximately 20 000, i.e., slightly higher than that of Prodan,[19] which is another commonly used solvatochromic fluorophore. Moreover, all compounds exhibited high fluorescence quantum yields (Φ_{FL} > 0.90) in nonpolar solvents such as hexane and toluene, which could be related to their remarkable photostability in solution (vide infra). The sensitivity of the fluorescence wavelength to the polarity of the solvent followed the order **PA1** > **PA18** ≈ **P16** > **PA13** > **PA138**.

The results of the DFT/TD-DFT calculations suggested for all compounds a main S_0–S_1 transition with a transition moment along the long axis of the pyrene ring, even though the direction of the dipole moment strongly depends on the

DOI: 10.1021/acs.joc.5b01987
J. Org. Chem. 2015, 80, 10794–10805

particular DA substitution. Moreover, in the vacuum phase, all compounds possess $\pi-\pi^*$ first singlet excited states ($S_1(\pi-\pi^*)$), and no clear singlet and/or triplet $n-\pi^*$ excited states were observed near $S_1(\pi-\pi^*)$ (Figure S20–S29 and Table S13–S17).

Below, the photophysical properties of **PA1** and **PA13** are discussed in detail as these exhibited exceptional behavior.

*Photophysical Properties of **PA1**.* As shown in Figure 2 and Table 1, **PA1** exhibited a fluorescence that changed from green (λ_{em} = 520 nm) in hexane to red (λ_{em} = 643 nm) in methanol with high Φ_{FL} values (hexane: 0.90; methanol: 0.55). Among **PA1**, **PA18**, **P16**, **PA13**, and **PA138**, **PA1** exhibited the most intense brightness and sensitivity to solvent polarity.

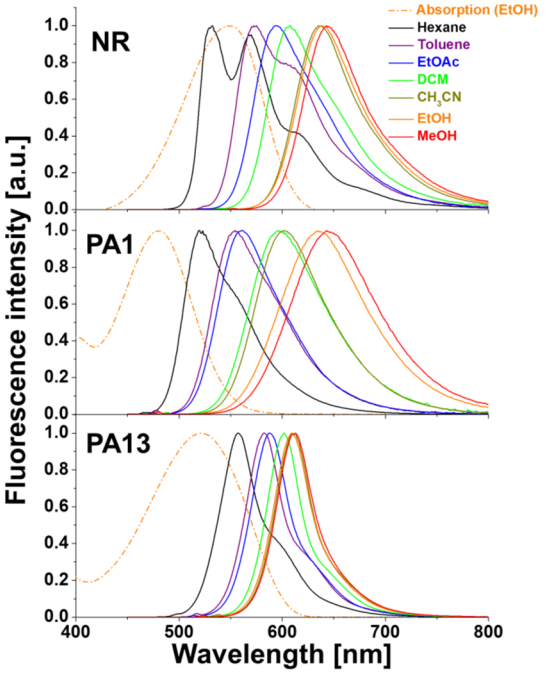

Figure 2. Absorption and fluorescence spectra of **NR**, **PA1**, and **PA13** in organic solvents of different polarity (5 μM, λ_{ex}= $\lambda_{abs,max}$). Absorption extinction coefficients of 42 000, 21 000, and 20 000 were measured for ethanol solutions of **NR**, **PA1**, and **PA13**, respectively.

Interestingly, **PA1** maintained high Φ_{FL} values for all solvents tested. This behavior is unusual for solvatochromic fluorophores, because the Φ_{FL} of solvatochromic dyes typically decreases in nonpolar and/or highly polar solvents.[29] This finding can be explained by our previous discussion regarding the simple D–π–A-shaped pyrene **PA**:[19] the results of the DFT/TD-DFT calculations imply that the S_1 of **PA1** maintains pure ($\pi-\pi^*$) character and is removed from the $T_n(n-\pi^*)$ state even in nonpolar solvents, which decreases the energy gap between ($\pi-\pi^*$) and ($n-\pi^*$) (Figure S20, S21 and Table S13). This suggests that the intersystem crossing (ISC) based on *El-Sayed's rule*[30] is inefficient, and therefore, **PA1** exhibits a high Φ_{FL} in apolar solvents. This discussion should equally apply to the other new dyes (Figure S22–S29 and Table S17–S17). The reason for the high Φ_{FL} of **PA1** in polar solvents is the moderate change in the dipole moment ($\Delta\mu$) of **PA1** between the ground and excited states ($\Delta\mu$ = 6.6 D, estimated by the Lippert–Mataga equation;[31] see Figure S12), relative to those of solvatochromic dyes such as the fluorene analogue of Prodan ($\Delta\mu$ = 12 D), whose Φ_{FL} is known to decrease with increasing solvent polarity.[32] This indicates that the thermal deactivation (internal conversion) based on the *energy-gap rule*[33] is also inefficient, which means that **PA1** is able to maintain a high Φ_{FL} in polar and nonpolar solvents. On the basis of this notion, **PA1** might be regarded as a "modified" **PA**, owing to the introduction of donors at the 3- and 8-positions that shift the absorption and fluorescence wavelength bathochromically.

Another interesting feature of **PA1** is its similar fluorescence wavelength and sensitivity to polarity when compared to **NR**. Even though the Φ_{FL} values of both are comparable, the absorption coefficient of **PA1** is only approximately half of that of **NR**; hence, the brightness of **PA1** is also ca. half of that of **NR**. However, taking into account that **PA1** exhibits a larger Stokes shift and that its photostability in toluene is eight times higher than that of **NR** (vide infra), **PA1** might find applications as an environmentally sensitive fluorescent probe.

*Photophysical Properties of **PA13**.* Interestingly, **PA13** exhibited an absorption wavelength around 520 nm, which is significantly red-shifted (~40 nm) relative to the other pyrene derivatives. According to the results of the DFT/TD-DFT calculations, only **PA13** exhibits a dipole moment along the transition moment of the new dyes (Figure S22 and S23), suggesting that a relatively strong charge transfer (CT) characteristic should appeared on the red-shifted S_0-S_1 transition. In fact, **PA18**, which exhibits a dipole moment perpendicular to a transition moment, showed both experimentally and theoretically a relatively short absorption wavelength (Figure S11, S26 and S27). The results of the DFT/TD-DFT calculations furthermore imply that **PA13**

Table 1. Spectroscopic Properties of NR, PA1, and PA13

		$\lambda_{abs,max}$ [nm]			$\lambda_{em,max}$ [nm]			Φ_{FL}		
solvent	$E_T(30)$[a]	**NR**	**PA1**	**PA13**	**NR**	**PA1**	**PA13**	**NR**	**PA1**	**PA13**
hexane	31	508	466	498	532	520	557	0.55	0.94	0.93
toluene	33.9	524	478	516	572	554	582	0.84	0.96	0.94
dioxane	36	519	476	512	582	557	585	0.86	0.96	0.92
EtOAC	38.1	524	475	514	594	562	587	0.88	0.94	0.93
DCM	40.7	539	489	534	608	597	602	0.88	0.93	0.91
acetone	42.2	533	477	521	614	581	598	0.88	0.95	0.90
DMSO	45.1	552	490	535	635	601	609	0.80	0.91	0.75
CH_3CN	45.6	535	482	525	620	596	602	0.85	0.93	0.88
EtOH	51.9	549	480	522	638	635	609	0.62	0.64	0.87
MeOH	55.4	553	480	523	643	643	613	0.46	0.50	0.83

[a]The values for the polarity index, $E_T(30)$, were obtained from ref 36.

DOI: 10.1021/acs.joc.5b01987
J. Org. Chem. 2015, 80, 10794–10805

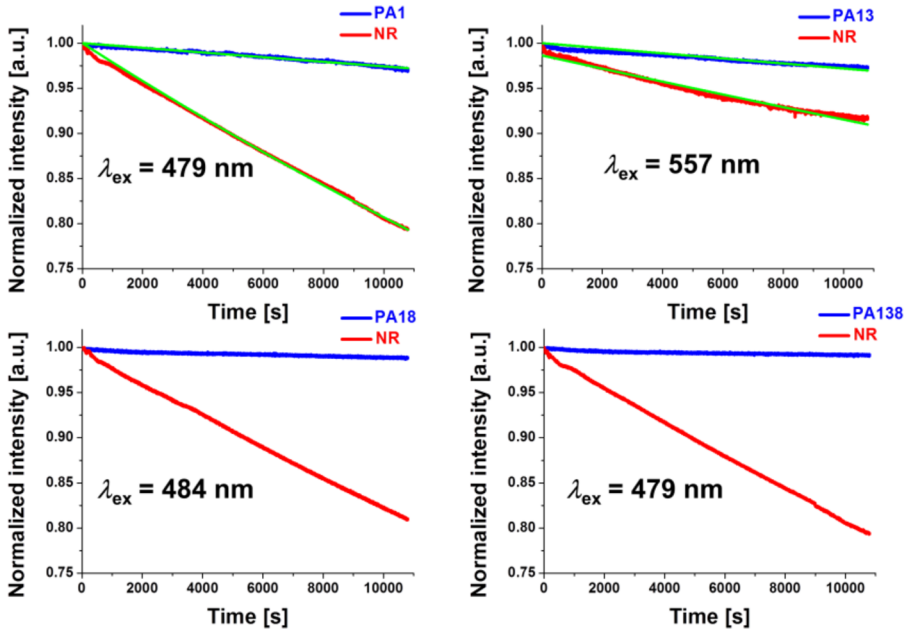

Figure 3. Photodegradation of **PA1**, **PA13**, **PA18**, and **PA138** (blue lines) and **NR** (red lines) in toluene. Excitation wavelengths (λ_{ex}) were obtained from the cross point of the absorption spectra between each of the new dyes and **NR** in 5 μM solution. The curves for **PA1** and **PA13** were fitted with a single exponential decay function (green lines): $I = y_0 + \exp(-t/\tau_p)$, where $y_0 = 0$ (final intensity after total photobleaching), τ_p is the degradation constant, I the measured fluorescence intensity, and t the time of experiment.

contains a large $\Delta\mu$. However, the spectroscopic measurement showed an opposite behavior, i.e., a less prominent solvatochromic behavior of **PA13**. This observation contradicted our expectations, and the detailed fluorescence mechanism of **PA13** still remains unclear. Importantly, the observed results indicated that the structure of **PA13** should be capable to efficiently decrease the optical band gap of pyrene. Such information would be highly useful for energy-gap engineering purposes, which is reflected in the fact that several researchers have investigated the relationship between structure and optoelectronic properties of pyrene derivatives.[16]

Another interesting characteristic of **PA13** is that its fluorescence is accompanied by a high Φ_{FL} value and a relatively narrow band in all the solvents tested. The observed narrow fluorescence band might be related to the small Stokes shift of **PA13**.[34] The results of the DFT/TD-DFT calculations indicated that **PA13** exhibits a particularly low intramolecular reorganization energy (0.26, 0.42, 0.42, and 0.46 eV for **PA13**, **PA1**, **PA138**, and **PA18**, respectively) (Table S13−S17). One of the reasons why **PA13** has a high Φ_{FL} value should be related to its moderate solvatochromic behavior. As previously discussed, **PA13** should have a small $\Delta\mu$ value, and the internal conversion quenching based on the *energy-gap rule* should accordingly be inefficient. From a functional materials perspective, such properties present two possibilities for **PA13**. The first is that **PA13** could be applied as a FRET donor, which would require a stable fluorescence position. In fact, only a limited number of dyes exist that exhibit an excitation around 500 nm and simultaneously an emission around 600 nm. Second, the structure of **PA13** should be useful for the development of a two photon-active fluorophore. Although such dyes are required to exhibit efficient two-photon absorption and subsequent fluorescence in the longer wavelength region, i.e., in the optical tissue window (650−1100 nm),[35] the currently applied D/A concept often causes the fluorescence to broaden and become thus inefficient. As this is not the case for **PA13**, this pyrene derivative may help to address this problem.

Photophysical Properties of PA16, PA18, and PA138. **PA16** and **PA18** exhibited similar Φ_{FL} and fluorescence behavior in terms of sensitivity to solvent polarity (Figure S11 and Table S1). Both of them showed an intermediate solvatochromic response relative to **PA1** and **PA13**. The solvatochromism of **PA16**, despite its electronically symmetric structure, should most likely be attributed to the "symmetry breaking" of quadrupole molecules.[37] In highly polar solvents, including hydrogen-bond acceptor solvents such as dimethyl sulfoxide (DMSO), **PA16** and **PA18** suffered from drastic fluorescence deactivation. Their solvatochromic behavior suggested that the $\Delta\mu$ values of **PA16** and **PA18** should be smaller than that of **PA1**. Therefore, the observed fluorescence quenching in highly polar solvents should not be derived from typical dipole−dipole interactions, but from other specific solvent−solute interactions (vide infra). Moreover, a clear solvatochromic fluorescence could not be observed for **PA138**. In general, the sensitivity of the fluorescence wavelength of D/A pyrene derivatives to the polarity of the solvent decreased with increasing number of acceptor groups on the pyrene core. Except for **PA13**, the brightness of the D/A pyrene derivatives also decreased with increasing number of acceptor groups on the pyrene. This is probably related to the potential role of a formyl group might play in the context of quenching. Certain molecules that contain a formyl group have shown that the formyl group may cause intramolecular rotation and subsequent internal conversion quenching.[38] Such a behavior might be promoted in DMSO, as DMSO is able the cleave and/or prevent inherent hydrogen bonding between pyrene and each formyl group and thus accelerate intramolecular rotation.[29] Regardless, the exact reasons why the substitution with acceptor groups renders D/A pyrene derivatives less sensitive to solvent polarity and why **PA13** is so bright in contrast to **PA16**, **PA18** and **PA138** still remain unclear.

DOI: 10.1021/acs.joc.5b01987
J. Org. Chem. 2015, 80, 10794−10805

However, the above discussion suggests that **PA16**, **PA18**, and **PA138** should be, at least at the moment, less attractive emitting materials. Nevertheless, considering the facile preparation of **PA16** and **PA18**, they should be expected to constitute useful building blocks for future derivatizations.

Photostability. The photostability of the new dyes was evaluated by recording their photodegradation curves in toluene and comparing them to that of **NR**, which is considered to be a highly photostable solvatochromic fluorophore.[39] Toluene was selected as a solvent, as the photostability of solvatochromic dyes usually decreases in apolar solvents.[32] This is a crucial problem especially for applications in apolar media, e.g., in lipid membranes of living cells.[18d] In these photostability measurements, different excitation wavelengths were used. These corresponded to a cross point between the absorption spectra of each new dye and that of **NR** at the same concentration, in order to enable direct comparison between each dye and **NR**. Surprisingly, all compounds exhibited a higher photostability than **NR** under continuous photoexcitation for 3 h (Figure 3 and Table 2). For example, when

Table 2. Photostability of PA1, PA13, PA18, and PA138 and NR in Toluene (rt, 5 μM)

dye	λ_{ex} [nm]	O.D.[a]	τ_p [min]	R [%][b]
PA1			6395	97
PA138	479	0.12	N.D.[c]	99
NR			777	79
PA13	557	0.053	5852	97
NR			2231	91
PA16	475	0.11	N.D.[c]	99
NR			813	80
PA18	484	0.13	N.D.[c]	99
NR			850	81

[a]O.D. refers to the optical density. [b]R is the remaining fluorescence intensity after 3 h of excitation. [c]Not determined due to little photodegradation.

PA1 and **NR** were excited at 479 nm, **PA1** lost only 3% of its initial fluorescence intensity, while **NR** lost more than 20%. The values of the time constant of photodegradation (τ_p) for **PA1** (τ_p = 6395 min) and **NR** (τ_p = 777 min) were estimated by fitting a single exponential decay function, and indicated that the photostability of **PA1** is eight times higher than that of **NR**. According to a recent report by Blanchard et al.,[40] photobleaching is mainly caused by reactive species such as singlet oxygen, which are generated by energy and/or electron transfer from the excited triplet state of the dye to molecular oxygen. This means that dyes with lower ISC rate constants tend to be photostable, unless they show photoisomerization or unexpected multiphoton absorption. Considering that **PA1**, **PA13**, **PA18**, and **PA138** show high Φ_{FL} values (>0.90 even in nonpolar solvents), which generally induce a higher degree of ISC compared to **NR** (Φ_{FL} = 0.55 in hexane), they might have lower ISC rate constants and therefore be much more photostable than **NR**. In fact, a correlation between high Φ_{FL} values in nonpolar solvents and photostability can be found in a report by Klymchenko et al.[32] It is worth pointing out that the above discussion should be very important in order to understand the advantage of using pyrene as a building block for optoelectronic materials, which would help to overcome crucial drawbacks of existing fluorophores with a D−π−A structure.

Single-Molecule Characterization of PA1. As **PA1** showed the most promise as a fluorescent probe among all the new dyes, we tested the photophysical properties of **PA1** on the single-molecule level. We also compared the single-molecule characteristics of **PA1** with those of **NR**, as the latter has been employed as an environmentally sensitive single-molecule fluorophore.[41]

As shown in Figure 4a, single molecules of **PA1** dispersed in thin poly(methyl methacrylate) (PMMA) films were readily

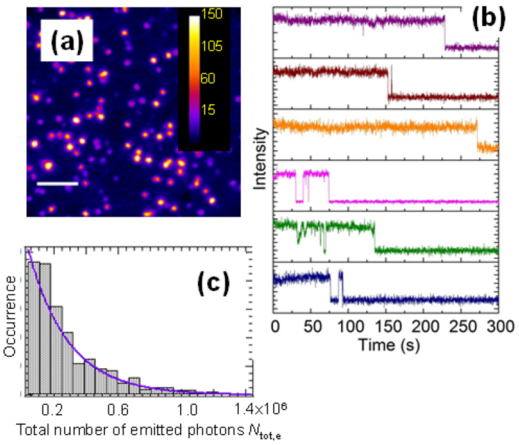

Figure 4. Single-molecule characterization of **PA1** in a PMMA matrix. (a) Fluorescence image of single **PA1** molecules (sum of 300 consecutive frames); the color bar shows the total number of photons ($\times 10^{-3}$) detected for each pixel in 30 s. The scale bar represents 4 μm. (b) Representative fluorescence intensity traces for six individual molecules, showing fluorescence intermittency (blinking) and single-step photobleaching. (c) Distribution of the total number of photons emitted before photobleaching; $N_{tot,e}$, was obtained from the analysis of 416 molecules. The solid line represents the corresponding single-exponential fitting.

detectable in an epifluorescence image, showing good contrast and signal-to-noise ratio. Figure 4b shows representative fluorescence intensity traces for six individual molecules undergoing fluorescence intermittency (blinking) and single-step photobleaching. For comparison, intensity traces for single molecules of **NR** are shown in Figure S14. The comparison revealed that single molecules of **PA1** appear to be more stable and less susceptible to blinking than single molecules of **NR**. A statistical estimate on an ensemble of single molecules showed that ca. 28% of **PA1** molecules underwent blinking in the first 100 s of the measurement, compared to 37% of the **NR** molecules. The overall photostability on the single-molecule level was analyzed by measuring the total number of photons emitted before the photobleaching for each molecule was studied, and by plotting a distribution of the number of emitted photons for a statistical ensemble of 416 **PA1** molecules (Figure 4c). Assuming that the photobleaching event is a photochemical reaction of first order, the distribution curve was fitted by a single-exponential function to obtain the average value for the total number of photons emitted ($N_{tot,e}$). The same analysis was carried out for single molecules of **NR** (Figure S14). $N_{tot,e}$ values of 250 000 and 190 000 photons were obtained for **PA1** and **NR**, respectively, showing that the photostability of **PA1** on the single-molecule level in a solid polymer matrix is 1.3 times higher than that of **NR**. The difference in photostability between a single molecule and a solution of the dye can be derived from the quantity and/or

DOI: 10.1021/acs.joc.5b01987
J. Org. Chem. 2015, 80, 10794−10805

diffusion rate of oxygen in the system, or from the different mechanisms (photochemical reactions) in solution and the polymer solid-state. It may be concluded that **PA1** exhibits the highest $N_{tot,e}$ value and photostability on the single-molecule level in this class of reported solvatochromic fluorophores, which provides further motivation to develop better fluorophores based on pyrene.

CONCLUSION

We demonstrated the first systematic and efficient synthesis of five 1-, 3-, 6-, and 8-tetrasubstituted pyrene derivatives with asymmetric D/A patterns (**PA1**, **PA18**, **P16**, **PA13**, and **PA138**). The successful synthesis of **PA13** is an important achievement, as even simple modifications of substituents at the 1- and 3-positions are nontrivial without protecting the 7-position. We also examined the photophysical properties of **PA1**, **PA18**, **P16**, **PA13**, and **PA138** in order to understand the relationship between their structure and electronic properties. We found that **PA1** shows promising fluorescence properties: it exhibited strong and bright solvatochromic fluorescence over a wide polarity range and displayed higher photostability than **NR**. In addition, we showed that **PA13** exhibits an absorption band with an exceptionally large red shift, together with bright and narrow, but less solvatochromic fluorescence. This information should be very important for the development of materials with engineered energy gaps and nonlinear optical materials such as two photon-active fluorophores. Remarkably, we found that all new pyrene derivatives exhibited much higher photostability than **NR**, which rationalized in terms of the specific inefficiency of their ISC. This highlights a further advantage of these new dyes and also provides important information in order to overcome the limited photostability of existing dipole fluorophores.

It is possible to further derivatize and modify **PA1**, **PA18**, **P16**, **PA13**, and **PA138**, as they, or their synthetic intermediates, are able to participate in several reactions, including transition metal-mediated catalysis and functional group transformations. This should be useful for the development of functionalized pyrene-based D/A derivatives that may be used as synthons for a broad variety of new materials. Although several phenomena, especially with respect to the photophysical properties of **PA13**, remain to be clarified we believe that the results presented here should be of great interest to the wider materials science community.

EXPERIMENTAL SECTION

Synthesis of 3,6,8-Tri(piperidin-1-yl)pyrene-1-carbaldehyde (PA1). Over a period of 15 min, bromine (3.2 g, 20 mmol) was added dropwise under vigorous stirring to a solution of 1-formylpyrene (1.2 g, 5.1 mmol) in nitrobenzene (30 mL) at 120 °C. The mixture was kept at 120 °C for 4 h, before being allowed to cool to room temperature. The precipitate was filtered off, washed with ethanol and chloroform, and dried in vacuo to afford **2** as a yellow powder (2.3 g, 95%). Because of its low solubility, the product was used in the next step without further purification or characterization. Subsequently, a mixture of **2** (0.70 g, 1.5 mmol), cesium carbonate (2.1 g, 6.3 mmol), $Pd(OAc)_2$ (50 mg, 0.23 mmol), RuPhos (0.21 g, 0.45 mmol) in toluene (25 mL) was stirred for 15 min at 100 °C under an atmosphere of argon. Then, piperidine (0.53 mL, 5.4 mmol) was added to the solution and the resulting mixture was stirred for 6 h. After the mixture was cooled to room temperature, chloroform was added and the insoluble parts were removed by filtration. The resulting solution was washed with brine, dried over $MgSO_4$, and filtered. All volatiles were removed in vacuo and the residue was subjected to column chromatography on silica gel using chloroform, followed by a recrystallization from methanol to afford **PA1** as a red powder (150 mg, 20%): mp 198.5−200.5 °C; ^{1}H NMR (400 MHz, $CDCl_3$) δ 10.79 (s, 1H), 9.05 (d, J = 9.5 Hz, 1H), 8.46 (d, J = 9.4 Hz, 1H), 8.40 (d, J = 9.5 Hz, 1H), 8.26 (d, J = 9.4 Hz, 1H), 8.10 (s, 1H), 7.43 (s, 1H), 3.31−3.09 (m, 12H), 1.99−1.84 (m, 12H), 1.79−1.64 (m, 6H); ^{13}C NMR (100 MHz, $CDCl_3$) δ 192.8, 151.9, 151.6, 147.6, 131.6, 129.6, 127.8, 127.7, 126.5, 126.3, 125.4, 121.0, 120.8, 120.5, 120.2, 119.4, 109.2, 55.6, 55.5, 55.0, 27.1, 27.0, 25.0, 24.9; HRMS (FAB) Calcd for $C_{32}H_{37}N_3O$ 479.2937, found 479.2935 ([M]$^+$).

General Procedure for a Gram-Scale Synthesis of Pyrene-1,6-dicarbaldehyde (4b), and Pyrene-1,8-dicarbaldehyde (4c). A solution of *n*-butyllithium in hexane (2.6 M, 6 equiv) was added dropwise to a solution of 1,6- or 1,8-dibromopyrene in anhydrous THF under an atmosphere of argon at 0 °C. After the reaction mixture was stirred for 1 h at this temperature, DMF (6 equiv) was added dropwise to the solution. The mixture was stirred at room temperature for 1 h before water was added. The resulting precipitation was filtered off and washed consecutively with water, methanol, and warm toluene to afford the targeted diformylpyrenes **4b** (2.3 g, 66%) and **4c** (1.9 g, 55%), respectively.

4b: ^{1}H NMR (300 MHz, $CDCl_3$) δ 10.84 (s, 2H), 9.62 (d, J = 9.4 Hz, 2H), 8.57 (d, J = 7.9 Hz, 2H), 8.54 (d, J = 7.9 Hz, 2H), 8.28 (d, J = 9.4 Hz, 2H).

4c: ^{1}H NMR (300 MHz, $CDCl_3$) δ 10.87 (s, 2H), 9.62 (s, 2H), 8.56 (d, J = 7.4 Hz, 2H), 8.40 (d, J = 7.9 Hz, 2H), 8.26 (s, 2H).

Large-Scale Synthesis of 3,8-Di(piperidin-1-yl)pyrene-1,6-dicarbaldehyde (PA16) and 1,8-Di(piperidin-1-yl)pyrene-3,6-dicarbaldehyde (PA18). *General Dibromination Procedure for **4b** and **4c** and Subsequent Protection of the Formyl Groups As Dimethylacetals (Synthesis of **5b** and **5c**).* Over a period of 15 min and under vigorous stirring, bromine (4 equiv) was added dropwise to a solution of **4b** or **4c** (1 g, 4.0 mmol) in 100 mL of dichloromethane at 40 °C. The mixture was kept at 40 °C for 2 h, before 100 mL of methanol were added and heating to reflux was maintained for 1 h. After cooling, the resulting precipitate was collected by filtration, washed with methanol, and dried in vacuo to afford the targeted diformylpyrenes **5b** (1.1 g, 54%) and **5c** (1.3 g, 64%), respectively.

*1,6-Dibromo-3,8-bis(dimethoxymethyl)pyrene (**5b**).* ^{1}H NMR (300 MHz, $CDCl_3$) δ 8.60 (s, 2H), 8.58 (d, J = 9.6 Hz, 2H), 8.53 (d, J = 9.6 Hz, 2H), 6.23 (s, 2H), 3.50 (s, 12H); LRMS (FAB) Calcd for $C_{22}H_{20}Br_2O_4$ 505.9728, found 506 ([M]$^+$).

*1,8-Dibromo-3,6-bis(dimethoxymethyl)pyrene (**5c**).* ^{1}H NMR (300 MHz, $CDCl_3$) δ 8.39 (s, 2H), 8.36 (s, 2H), 6.64 (s, 2H), 5.89 (s, 2H), 3.56 (s, 6H), 3.34 (s, 6H); LRMS (FAB) Calcd for $C_{22}H_{20}Br_2O_4$ 505.9728, found 506 ([M]$^+$).

*Synthesis of **PA16** and **PA18**: General Procedure for the Buchwald−Hartwig Amination of **5b** and **5c** and the Subsequent Deprotection of the Dimethylacetal Moieties.* A mixture of **5b** or **5c**, sodium *tert*-butoxide (2.8 equiv), $Pd(OAc)_2$ (10 mol %), and BINAP (20 mol %) in toluene was stirred for 15 min at 100 °C under an atmosphere of argon. Subsequently, piperidine (2.4 equiv) was added to the solution and the resulting mixture was stirred for 12 h. After the mixture was cooled to room temperature, chloroform was added to the mixture and the insoluble parts were removed by filtration. The solution thus obtained was washed with brine, dried over $MgSO_4$, and filtered. The solvents were removed in vacuo and the residue was dissolved in THF/H_2O (5:1, v/v), before 10 mol % of *p*-toluenesulfonic acid monohydrate were added to this solution. The mixture was stirred at 70 °C for 2 h, before being extracted with chloroform, washed with brine, dried over $MgSO_4$, and filtered. The solvents were evaporated in vacuo, before the resulting residue was purified by column chromatography on silica gel (chloroform:hexane = 2:1) and a subsequent recrystallization from hexane/dichloromethane to afford diformylpyrenes **PA16** (0.17 g, 41%) and **PA18** (0.29 g, 58%), respectively.

PA16: Reddish solid; mp decomposed at T > 300 °C; ^{1}H NMR (300 MHz, $CDCl_3$) δ 10.86 (s, 2H), 9.36 (d, J = 9.5 Hz, 2H), 8.54 (d, J = 9.5 Hz, 2H), 8.20 (s, 2H), 3.29 (brs, 8H), 2.02−1.95 (brs, 8H), 1.77 (brs, 4H); ^{13}C NMR (100 MHz, $CDCl_3$) δ 192.9, 150.1, 129.5,

DOI: 10.1021/acs.joc.5b01987
J. Org. Chem. 2015, 80, 10794−10805

128.9, 127.7, 126.9, 124.9, 124.7, 121.7, 55.3, 27.0, 24.8; HRMS (FAB) Calcd for $C_{28}H_{28}N_2O_2$ 424.2151, found 424.2157 ([M]$^+$).

PA18: Reddish solid; mp decomposed at T > 300 °C; ^{1}H NMR (300 MHz, $CDCl_3$) δ 10.87 (s, 2H), 9.18 (s, 2H), 8.54 (s, 2H), 8.18 (s, 2H), 3.27 (brs, 8H), 2.03−1.96 (brs, 8H), 1.78 (brs, 4H); ^{13}C NMR (100 MHz, $CDCl_3$) δ 192.6, 150.3, 130.0, 128.6, 127.3, 126.9, 125.5, 123.6, 120.8, 55.3, 27.0, 24.9; HRMS (FAB) Calcd for $C_{28}H_{28}N_2O_2$ 424.2151, found 424.2157 ([M]$^+$).

Synthesis of 8-Bromopyrene-1,3,6-tricarbaldehyde (7). A 2.6 M solution of *n*-butyllithium in hexane (1.3 mL, 3.4 mmol) was added dropwise to a solution of **5b** (1.45 g, 2.85 mmol) in anhydrous THF (30 mL) at −50 °C under an atmosphere of argon. After the reaction mixture was stirred for 30 min at this temperature, DMF (0.34 mL, 3.4 mmol) was added dropwise to the solution. The mixture was warmed to room temperature and stirred for 30 min. After adding water to quench the reaction, the organic layer was extracted with chloroform, washed with brine, dried over $MgSO_4$, and filtered. Subsequently, the methyl acetal groups of **5b** were directly deprotected. After the solvents were removed in vacuo, the resulting residue was dissolved in THF/H_2O (5:1, v/v), before 10 mol % of *p*-toluenesulfonic acid monohydrate were added to the solution. The mixture was stirred at 70 °C for 2 h. The obtained precipitate was filtered, washed with THF, and dried in vacuo to afford 7 (0.38 g, 37%), which was, on account of its low solubility, used in the next step without further purification or characterization. Orange powder; LRMS (FAB) Calcd for $C_{19}H_9BrO_3$ 363.9735, found 365 ([M + H]$^+$).

Synthesis of 8-(Piperidin-1-yl)pyrene-1,3,6-tricarbaldehyde (PA138). A mixture of 7 (0.30 g, 0.82 mmol), cesium carbonate (0.38 g, 1.2 mmol), $Pd(OAc)_2$ (9.2 mg, 0.041 mmol), and RuPhos (57 mg, 0.12 mmol) in toluene (5 mL) was stirred for 15 min at 100 °C under an atmosphere of argon. Subsequently, piperidine (0.097 mL, 0.99 mmol) was added to the solution and the resulting mixture was stirred for 2 h. After the mixture was cooled to room temperature, chloroform was added to the mixture and the insoluble parts were removed by filtration. The obtained solution was washed with brine, dried over $MgSO_4$, and filtered. All volatiles were removed in vacuo and the obtained residue was subjected to column chromatography on silica gel using chloroform/hexane (5:1, v/v), followed by recrystallization from ethanol to afford **PA138** (120 mg, 40%). Violet powder; mp decomposed at T > 300 °C; ^{1}H NMR (400 MHz, $CDCl_3$) δ 10.95 (s, 1H), 10.86 (s, 1H), 10.80 (s, 1H), 9.63 (d, J = 9.5 Hz, 1H), 9.55 (s, 2H), 8.92 (s, 1H), 8.82 (d, J = 9.5 Hz, 1H), 8.29 (s, 1H), 3.39 (brs, 4H), 2.01 (m, 4H), 1.80 (m, 2H); ^{13}C NMR (100 MHz, $CDCl_3$) δ 192.5, 192.2, 152.7, 138.2, 135.0, 134.5, 130.8, 129.9, 129.0, 127.8, 127.5, 127.3, 125.9, 125.8, 125.5, 124.7, 123.6, 121.8, 55.6, 26.8, 24.7; HRMS (FAB) Calcd for $C_{24}H_{19}NO_3$ 369.1365, found 369.1360 ([M]$^+$).

Synthesis of 3-Bromopyrene-1-carbaldehyde (8a), 6-Bromopyrene-1-carbaldehyde (8b), and 3-Bromopyrene-1-carbaldehyde (8c). *N*-bromosuccinimide (8.5 g, 47.8 mmol) was added to a solution of 1-formylpyrene (10 g, 43.4 mmol) in 150 mL of DMF. The mixture was heated to reflux for 3 h, before 200 mL of water were added. The resulting precipitate was collected by filtration, washed with methanol, and dried in vacuo to afford a mixture of **8a**, **8b**, and **8c** (13 g, 97%). These crude products were used in next step without further purification. The reaction progress was monitored by ^{1}H NMR spectroscopy of the mixture, measuring the integration ratio between hydrogen resonances derived from the formyl groups at 10.8 ppm and resonances from aromatic hydrogens (Figure S4). Yellow solid; LRMS (EI) Calcd for $C_{17}H_9BrO$ 307.9837, found 308 ([M]$^+$).

Synthesis of 1-Bromo-3-(dimethoxymethyl)pyrene (9a), 1-Bromo-6-(dimethoxymethyl)pyrene (9b), and 1-Bromo-8-(dimethoxymethyl)pyrene (9c). A solution of **8a−c** (13 g, 42.1 mmol) in 250 mL of chloroform/methanol (1:1, v/v) was treated with *p*-toluenesulfonic acid monohydrate (0.80 g, 4.2 mmol). After the mixture was heated to reflux for 2 h, potassium carbonate (10 g) was added to the mixture and stirring was continued for 30 min. After cooling, all solvents were removed in vacuo, before the resulting residue was dissolved in chloroform and filtered. The solvent was removed in vacuo and the resulting residue was passed through a short plug of silica (chloroform) to afford a mixture of **2a**, **2b**, and **2c** (13.1 g, 88%). Reaction progress was confirmed by ^{1}H NMR spectroscopy of the mixture, measuring the integration ratio between hydrogen resonances derived from the benzyl moiety (∼6 ppm) and aromatic hydrogen resonances, as well as from the disappearance of the peak associated with the formyl groups (Figure S4). Yellow solid; LRMS (FAB) Calcd for $C_{19}H_{15}BrO_2$ 354.0255, found 354 ([M]$^+$).

Synthesis of Pyrene-1,3-dicarbaldehyde (4a), Pyrene-1,6-dicarbaldehyde (4b), and Pyrene-1,8-dicarbaldehyde (4c). A 2.6 M solution of *n*-butyllithium in hexane (27.7 mL, 72.0 mmol) was added dropwise to a mixture of **9a−c** (12.8 g, 36.0 mmol) in anhydrous THF (200 mL) at −50 °C under an argon atmosphere. After the reaction mixture was stirred for 1 h at this temperature, DMF (5.6 mL, 72.0 mmol) was added dropwise. The mixture was warmed to room temperature, where stirring was continued for 1 h. After adding water, the mixture was extracted with chloroform, washed with water, dried over $MgSO_4$, and filtered. All volatiles were removed in vacuo to afford **10a−c**. Subsequently, a mixture of **3a−c** was dissolved in 200 mL of THF/H_2O (5:1, v/v), before *p*-toluenesulfonic acid monohydrate (0.68 g, 3.6 mmol) was added. The mixture was stirred at 70 °C for 2 h, extracted with chloroform, washed with brine, dried over $MgSO_4$, and filtered. The solvents were evaporated in vacuo, and the resulting residue was purified by column chromatography on silica gel (chloroform) to afford **4a−c** as yellow solids in a combined yield of 28%. The yield of **4a** (1.48 g, 16%), **4b** (4%), and **4c** (0.79 g, 8%) was estimated by ^{1}H NMR spectroscopy. Note on the separation of three structural isomers: The R_f values of **4a−c** in the column chromatography on silica gel (chloroform) decrease in the order **4b** > **4a** > **4c**, albeit that the differences are very small. Therefore, silica column chromatography serves only to roughly separate **4a−c** into two groups; one is the mixture of **4a** and **4b**, while the other consists of a mixture of **4a** and **4c**. However, an ensuing fractional recrystallization from chloroform was able to afford pure **4a−c** (Figure S5).

4a: ^{1}H NMR (300 MHz, $CDCl_3$) δ 10.83 (s, 2H), 9.57 (d, J = 9.4 Hz, 2H), 8.91 (s, 1H), 8.53 (d, J = 9.4 Hz, 2H), 8.48 (d, J = 7.7 Hz, 2H), 8.23 (t, J = 7.7 Hz, 1H).

Synthesis of Dimethyl pyrene-1,3-dicarboxylate (11a), Dimethyl pyrene-1,6-dicarboxylate (11b), and Dimethyl pyrene-1,8-dicarboxylate (11c). A solution of a mixture of **4a−c** (1.1 g, 4.3 mmol) in 70 mL of methanol/THF/chloroform (3:2:2, v/v/v) was treated with zinc bromide (0.19 g, 0.85 mmol) and hydrogen peroxide (35%, v/v, 3.3 g, 34.1 mmol). The mixture was heated to reflux for 12 h, before solvents were evaporated in vacuo. The resulting residue was dissolved in chloroform, washed with water, dried over $MgSO_4$, and filtered. All volatiles were evaporated in vacuo, before the residue was purified by column chromatography on silica gel (chloroform) to afford a mixture of **11a−c** (0.59 g, total yield: 44%). Reaction progress was monitored by ^{1}H NMR spectroscopy of the mixture, measuring the integration ratio between resonances derived from OMe (∼4.1 ppm) and aromatic resonances, as well as the disappearance of the peak associated with the formyl groups (Figure S6). Yellow solid; LRMS (FAB) Calcd for $C_{20}H_{14}O_4$ 318.0892, found 341 ([M + Na]$^+$). Note on the separation of three structural isomers: The R_f values of **11a−c** in the column chromatography on silica gel (chloroform) decrease in the order **11b** > **11a** > **11c**. Importantly, the isolation of **11c** from the mixture of **11a−c** by column chromatography on silica is much easier relative to the separation of **4a−c**.

Synthesis of Dimethyl 6,8-dibromopyrene-1,3-dicarboxylate (12a) and Dimethyl 3,8-dibromopyrene-1,6-dicarboxylate (12b). Under vigorous stirring, bromine (0.13 mL, 0.40 g, 2.5 mmol) was added dropwise over a period of 15 min to a solution of **11a** and **11b** (0.20 g, 0.63 mmol) in 20 mL of dichloromethane at 40 °C. The mixture was kept at 40 °C for 2 h, before 50 mL of methanol was added and the reaction mixture was heated to reflux for 1 h. After cooling, the resulting precipitation was collected by filtration, washed with methanol, and dried in vacuo to afford a mixture of **12a** and **12b** (0.19 g; total yield: 64%) The reaction progress was monitored by ^{1}H NMR spectroscopy of the mixture, measuring the integration ratio

DOI: 10.1021/acs.joc.5b01987
J. Org. Chem. 2015, 80, 10794−10805

between the signals arising from OMe (~4.1 ppm) and the aromatic resonances (Figure S7). Yellow solid; LRMS (FAB) Calcd for $C_{20}H_{12}Br_2O_4$ 473.9102, found 474 ([M]$^+$).

Synthesis of Dimethyl 6,8-di(piperidin-1-yl)pyrene-1,3-dicarboxylate (13a) and Dimethyl 3,8-di(piperidin-1-yl)pyrene-1,6-dicarboxylate (13b). A mixture of **12a** and **12b** (0.11 g, 0.23 mmol), cesium carbonate (0.21 g, 0.64 mmol), $Pd(OAc)_2$ (5.2 mg, 0.023 mmol), and RuPhos (21 mg, 0.046 mmol) in toluene was stirred for 15 min at 100 °C under an atmosphere of argon. Then, piperidine (55 μL, 0.55 mmol) was added and the resulting mixture was stirred for 6 h at this temperature. After the mixture was cooled to room temperature, chloroform was added and insoluble parts were removed by filtration. All solvents were evaporated in vacuo, before the resulting residue was purified by column chromatography on silica gel (chloroform) to afford a mixture of **13a** and **13b** (74 mg; combined yield: 66%) The reaction progress was monitored by ^{1}H NMR spectroscopy of the mixture, measuring the integration ratio between the resonances associated with OMe (~4.1 ppm), NCH_2- (~3.6 ppm), and the aromatic resonances (Figure S8). Orange solid; LRMS (FAB) Calcd for $C_{30}H_{32}N_2O_4$ 484.2362, found 507 ([M + Na]$^+$).

Synthesis of 6,8-Di(piperidin-1-yl)pyrene-1,3-dicarbaldehyde (PA13) and 3,8-Di(piperidin-1-yl)pyrene-1,6-dicarbaldehyde (PA16). A 1.0 M solution of DIBAL-H in toluene (0.60 mL, 0.60 mmol) was added dropwise to a mixture of **8a** and **8b** (71 mg, 0.15 mmol) in anhydrous THF (30 mL) at 0 °C under an atmosphere of argon. The reaction mixture was stirred for 1 h and the progress of the reaction was confirmed by TLC, before water was added. The mixture was carefully extracted with chloroform, washed with brine, dried over $MgSO_4$, and filtered. All solvents were evaporated in vacuo, and the resulting residue was dissolved in dichloromethane. This solution was treated with Dess–Martin periodinane (0.25 g, 0.60 mmol) and the mixture was stirred for 2 h at room temperature. After adding water, the mixture was extracted with chloroform, washed by water, dried over $MgSO_4$, and filtered. All solvents were removed in vacuo, and the resulting residue was purified by column chromatography on silica (chloroform) to afford a mixture of **PA13** and **PA16** (53 mg; combined yield: 85%). After separation of the structural isomers, each compound was purified by recrystallization from hexane. The ^{1}H NMR spectrum of **PA13** and **PA16** are shown in Figure S9. Note on the separation of three structural isomers: The order of the R_f values for **PA13** and **PA16** in the column chromatography on silica (chloroform) decreased in the order **PA16** > **PA13**, and ΔR_f was sufficient for the separation of the isomers.

PA13: Violet solid; mp decomposed at T > 300 °C; ^{1}H NMR (300 MHz, $CDCl_3$) δ 10.65 (s, 2H), 9.35 (d, J = 9.4 Hz, 2H), 8.70 (s, 1H), 8.67 (d, J = 9.4 Hz, 2H), 7.40 (s, 2H), 3.34 (brs, 8H), 2.02–1.95 (brs, 8H), 1.77 (brs, 4H); ^{13}C NMR (100 MHz, $CDCl_3$) δ 192.7, 155.2, 140.9, 136.5, 130.8, 127.0, 125.2, 119.7, 119.5, 109.3, 55.8, 26.9, 24.9; HRMS (FAB) Calcd for $C_{28}H_{28}N_2O_2$ 424.2151, found 424.2156 ([M]$^+$).

■ ASSOCIATED CONTENT

Supporting Information

The Supporting Information is available free of charge on the ACS Publications website at DOI: 10.1021/acs.joc.5b01987.

Additional experimental details. Results of the ^{1}H and/or ^{13}C NMR spectra of all compounds except for **2**. Absorption and fluorescence spectra, as well as spectroscopic properties for **PA16**, **PA18**, and **PA138**. Fluorescence lifetime decay profiles for **PA1**, **PA13**, **PA16**, **PA18**, and **PA138**. Results of DFT/TD-DFT calculations. (PDF)

■ AUTHOR INFORMATION

Corresponding Authors

*E-mail: nicosuke1004@gmail.com.

*E-mail: konishi.g.aa@m.titech.ac.jp.

Notes

The authors declare no competing financial interest.

■ ACKNOWLEDGMENTS

We thank Prof. Dr. Yusuke Tamaki and Prof. Dr. Osamu Ishitani (Tokyo Institute of Technology) for carrying out the fluorescence lifetime measurements. Y.N. was supported by a JSPS Fellowship for research abroad.

■ REFERENCES

(1) For the Ham effect, see: Kalyanasundaram, K.; Thomas, J. K. *J. Am. Chem. Soc.* **1977**, *99*, 2039–2044.

(2) For excimers, see: Turro, N. J.; Ramamurthyl, V.; Scaiano, J. C. *Modern Molecular Photochemistry of Organic Molecules*; University Science Books: Sausalito, CA, 2010; pp 253–255.

(3) (a) Winnik, F. M. *Chem. Rev.* **1993**, *93*, 587–614. (b) Martí, A. A.; Jockusch, S.; Stevens, N.; Ju, J.; Turro, N. J. *Acc. Chem. Res.* **2007**, *40*, 402–409. (c) Arrais, D.; Martins, J. *Biochim. Biophys. Acta, Biomembr.* **2007**, *11768*, 2914–2922. (d) Østergaard, M. E.; Hrdlicka, P. J. *Chem. Soc. Rev.* **2011**, *40*, 5771–5788. (e) Duhamel, D. *Langmuir* **2012**, *28*, 6527–6538. (f) Kraskouskaya, D.; Bancerz, M.; Soor, H. S.; Gardiner, J. E.; Gunning, P. T. *J. Am. Chem. Soc.* **2014**, *136*, 1234–1237. (g) Laguerre, A.; Stefan, L.; Larrouy, M.; Genest, D.; Novotna, J.; Pirrotta, M.; Monchaud, D. *J. Am. Chem. Soc.* **2014**, *136*, 12406–12414. (h) Niko, Y.; Konishi, G. *Macromolecules* **2012**, *45*, 2327–2337.

(4) (a) Figueira-Duarte, T. M.; Müllen, K. *Chem. Rev.* **2011**, *111*, 7260–7314. (b) Niko, Y.; Kawauchi, S.; Otsu, S.; Tokumaru, K.; Konishi, G. *J. Org. Chem.* **2013**, *78*, 3196–3207.

(5) (a) Yang, X. H.; Giovenzana, T.; Feild, B.; Jabbour, G. E.; Sellinger, A. *J. Mater. Chem.* **2012**, *22*, 12689–12694. (b) Chan, K. L.; Lim, J. P. F.; Yang, X.; Dodabalapur, A.; Jabbour, G. E.; Sellinger, A. *Chem. Commun.* **2012**, *48*, 5106–5108. (c) Thomas, K. R. J.; Kapoor, N.; Bolisetty, M. N. K. P.; Jou, J.-H.; Chen, Y.-L.; Jou, Y.-C. *J. Org. Chem.* **2012**, *77*, 3921–3932. (d) Kotchapradist, P.; Prachumrak, N.; Tarsang, R.; Jungsuttiwong, S.; Keawin, T.; Sudyoadsuk, T.; Promarak, V. *J. Mater. Chem. C* **2013**, *1*, 4916–4924. (e) Chercka, D.; Yoo, S.-J.; Baumgarten, M.; Kim, J.-J.; Müllen, K. *J. Mater. Chem. C* **2014**, *2*, 9083–9086. (f) Uchimura, M.; Watanabe, Y.; Araoka, F.; Watanabe, J.; Takezoe, H.; Konishi, G. *Adv. Mater.* **2010**, *22*, 4473–4478.

(6) (a) Zöphel, L.; Beckmann, D.; Enkelmann, V.; Chercka, D.; Rieger, R.; Müllen, K. *Chem. Commun.* **2011**, *47*, 6960–6962. (b) Kim, Y. S.; Bae, S. Y.; Kim, K. H.; Lee, T. W.; Hur, J. A.; Hoang, M. H.; Cho, M. J.; Kim, S.-J.; Kim, Y.; Kim, M.; Lee, K.; Lee, S. J.; Choi, D. H. *Chem. Commun.* **2011**, *47*, 8907–8909.

(7) (a) Lee, O. P.; Yiu, A. T.; Beaujuge, P. M.; Woo, C. H.; Holcombe, T. W.; Millstone, J. E.; Douglas, J. D.; Chen, M. S.; Fréchet, J. M. J. *Adv. Mater.* **2011**, *23*, 5359–5363. (b) Kim, J.-H.; Kim, H. U.; Kang, I.-N.; Lee, S. K.; Moon, S.-J.; Shin, W. S.; Hwang, D.-H. *Macromolecules* **2012**, *45*, 8628–8638. (c) Jeon, N. J.; Lee, J.; Noh, J. H.; Nazeeruddin, M. K.; Grätzel, M.; Seok, S. I. *J. Am. Chem. Soc.* **2013**, *135*, 19087–19090. (d) Lu, J.; Liu, S.; Li, H.; Shen, Y.; Xu, J.; Chengac, Y.; Wang, M. *J. Mater. Chem. A* **2014**, *2*, 17495–17501. (e) Kawata, S.; Pu, Y.-J.; Ohashi, C.; Nakayama, K.; Hong, Z.; Kido, J. *J. Mater. Chem. C* **2014**, *2*, 501–509. (f) Bathula, C.; Kim, M.; Song, C. E.; Shin, W. S.; Hwang, D.-H.; Lee, J.-C.; Kang, I.-N.; Lee, S. K.; Park, T. *Macromolecules* **2015**, *48*, 3509–3515.

(8) (a) Eddaoudi, M.; Kim, J.; Rosi, N.; Vodak, D.; Wachter, M.; O'Keeffe, M.; Yaghi, O. M. *Science* **2002**, *295*, 469–472. (b) Rowsell, J. L. C.; Yaghi, O. M. *J. Am. Chem. Soc.* **2006**, *128*, 1304–1315. (c) Wong-Foy, A. G.; Matzger, A. J.; Yaghi, O. M. *J. Am. Chem. Soc.* **2006**, *128*, 3494–3495. (d) Wan, S.; Guo, J.; Kim, J.; Ihee, H.; Jiang, D. *Angew. Chem., Int. Ed.* **2008**, *47*, 8826–8830. (e) Wan, S.; Guo, J.; Kim, J.; Ihee, H.; Jiang, D. *Angew. Chem., Int. Ed.* **2009**, *48*, 5439–5442. (f) Ronson, T. K.; League, A. B.; Gagliardi, L.; Cramer, C. J.; Nitschke, J. R. *J. Am. Chem. Soc.* **2014**, *136*, 15615–15624.

(9) (a) Merner, B. L.; Dawe, L. N.; Bodwell, G. J. *Angew. Chem., Int. Ed.* **2009**, *48*, 5487–5491. (b) Mochida, K.; Kawasumi, K.; Segawa, Y.; Itami, K. *J. Am. Chem. Soc.* **2011**, *133*, 10716–10719. (c) Yagi, A.;

DOI: 10.1021/acs.joc.5b01987
J. Org. Chem. 2015, 80, 10794–10805

Venkataramana, G.; Segawaa, Y.; Itami, K. *Chem. Commun.* **2014**, *50*, 957−959. (d) Iwamoto, T.; Kayahara, E.; Yasuda, N.; Suzuki, T.; Yamago, S. *Angew. Chem., Int. Ed.* **2014**, *53*, 6430−6434. (e) Singh, M.; Holzinger, M.; Tabrizian, M.; Winters, S.; Berner, N. C.; Cosnier, S.; Duesberg, G. S. *J. Am. Chem. Soc.* **2015**, *137*, 2800−2803.

(10) (a) Sagara, Y.; Kato, T. *Angew. Chem., Int. Ed.* **2008**, *47*, 5175−5178. (b) Sagara, Y.; Kato, T. *Nat. Chem.* **2009**, *1*, 605−610. (c) Diring, S.; Camerel, F.; Donnio, B.; Dintzer, T.; Toffanin, S.; Capelli, R.; Muccini, R.; Ziessel, R. *J. Am. Chem. Soc.* **2009**, *131*, 18177−18185. (d) Ma, M.; Kuang, Y.; Gao, Y.; Zhang, Y.; Gao, P.; Xu, B. *J. Am. Chem. Soc.* **2010**, *132*, 2719−2728. (e) Sagara, Y.; Komatsu, T.; Ueno, T.; Hanaoka, K.; Kato, T.; Nagano, T. *Adv. Funct. Mater.* **2013**, *23*, 5277−5284.

(11) (a) Kathayat, R. S.; Finney, N. S. *J. Am. Chem. Soc.* **2013**, *135*, 12612−12614. (b) Amendola, V.; Bergamaschi, G.; Boiocchi, M.; Fabbrizzi, L.; Mosca, L. *J. Am. Chem. Soc.* **2013**, *135*, 6345−6355. (c) Mosca, L.; Behzad, S. K.; Anzenbacher, P., Jr. *J. Am. Chem. Soc.* **2015**, *137*, 7967. (d) Lincoln, R.; Kohler, L.; Monro, S.; Yin, H.; Stephenson, M.; Zong, R.; Chouai, A.; Dorsey, C.; Hennigar, R.; Thummel, R. P.; McFarland, S. A. *J. Am. Chem. Soc.* **2013**, *135*, 17161−17175. (e) Moragues, M. E.; Toscani, A.; Sancenón, F.; Martínez-Máñez, R.; White, A. J. P.; Wilton-Ely, J. E. D. T. *J. Am. Chem. Soc.* **2014**, *136*, 11930−11933.

(12) (a) Yamato, T.; Fujimoto, M.; Nagano, Y.; Miyazawa, A.; Tashiro, M. *Org. Prep. Proced. Int.* **1997**, *29*, 321−330. (b) Figueira-Duarte, T. M.; Simon, S. C.; Wagner, M.; Druzhinin, S. I.; Zachariasse, K. A.; Müllen, K. *Angew. Chem., Int. Ed.* **2008**, *47*, 10175−10178.

(13) (a) Tashiro, M.; Yamato, T. *J. Am. Chem. Soc.* **1982**, *104*, 3701−3707. (b) Yamato, T.; Fujimoto, M.; Miyazawa, A.; Matsuo, K.; Yamato, T.; Fujimoto, M.; Miyazawa, A.; Matsuo, K. *J. Chem. Soc., Perkin Trans. 1* **1997**, 1201−1207. (c) Kawasumi, K.; Mochida, K.; Segawa, Y.; Itami, K. *Tetrahedron* **2013**, *69*, 4371−4374.

(14) (a) Crawford, A. G.; Dwyer, A. D.; Liu, Z.; Steffen, A.; Beeby, A.; Palsson, L.-O.; Tozer, D. J.; Marder, T. B. *J. Am. Chem. Soc.* **2011**, *133*, 13349−13362. (b) Crawford, A. G.; Dwyer, A. D.; Liu, Z.; Mkhalid, I. A. I.; Thibault, M.-H.; Schwarz, N.; Alcaraz, G.; Steffen, A.; Collings, J. C.; Batsanov, A. S.; Howard, J. A. K.; Mardera, T. B. *Chem. - Eur. J.* **2012**, *18*, 5022−5035. (c) Ji, L.; Edkins, R. M.; Lorbach, A.; Krummenacher, I.; Brückner, C.; Eichhorn, A.; Braunschweig, H.; Engels, B.; Low, P. J.; Marder, T. B. *J. Am. Chem. Soc.* **2015**, *137*, 6750−6753.

(15) (a) Hu, J.-Y.; Ni, X.-L.; Feng, X.; Era, M.; Elsegood, M. R. J.; Teat, S. J.; Yamato, T. *Org. Biomol. Chem.* **2012**, *10*, 2255−2262. (b) Feng, X.; Hu, J.-Y.; Iwanaga, F.; Seto, N.; Redshaw, C.; Elsegood, M. R. J.; Yamato, T. *Org. Lett.* **2013**, *15*, 1318−1321. (c) Zou, L.; Wang, X.-Y.; Shi, K.; Wang, J.-Y.; Pei, J. *Org. Lett.* **2013**, *15*, 4378−4381. (d) Feng, X.; Iwanaga, F.; Hu, J.-Y.; Tomiyasu, H.; Nakano, M.; Redshaw, C.; Elsegood, M. R. J.; Yamato, T. *Org. Lett.* **2013**, *15*, 3594−3597. (e) Zhang, S.; Qiao, X.; Chen, Y.; Wang, Y.; Edkins, R. M.; Liu, Z.; Li, H.; Fang, Q. *Org. Lett.* **2014**, *16*, 342−345.

(16) (a) Zöphel, L.; Enkelmann, V.; Müllen, K. *Org. Lett.* **2013**, *15*, 804−807. (b) Keller, S. N.; Veltri, N. L.; Sutherland, T. C. *Org. Lett.* **2013**, *15*, 4798−4801. (c) Ji, L.; Lorbach, A.; Edkins, R. M.; Marder, T. B. *J. Org. Chem.* **2015**, *80*, 5658−5665.

(17) (a) Saito, Y.; Shinohara, Y.; Ishioroshi, S.; Suzuki, A.; Tanaka, M.; Saito, I. *Tetrahedron Lett.* **2011**, *52*, 2359−2361. (b) Kim, H. M.; Lee, Y. O.; Lim, C. S.; Kim, J. S.; Cho, B. R. *J. Org. Chem.* **2008**, *73*, 5127−5130. (c) Niko, Y.; Cho, Y.; Kawauchi, S.; Konishi, G. *RSC Adv.* **2014**, *4*, 36480−36484.

(18) (a) Kivala, M.; Diederich, F. *Acc. Chem. Res.* **2009**, *42*, 235−248. (b) Pawlicki, M.; Collins, H. A.; Denning, R. G.; Anderson, H. L. *Angew. Chem., Int. Ed.* **2009**, *48*, 3244−3266. (c) Li, C.; Wonneberger, H. *Adv. Mater.* **2012**, *24*, 613−636. (d) Klymchenko, A. S.; Kreder, R. *Chem. Biol.* **2014**, *21*, 97−113. (e) Yang, Z.; Cao, J.; He, Y.; Yang, J. H.; Kim, T.; Peng, X.; Kim, J. S. *Chem. Soc. Rev.* **2014**, *43*, 4563−4601.

(19) Niko, Y.; Kawauchi, S.; Konishi, G. *Chem. - Eur. J.* **2013**, *19*, 9760−9765.

(20) Niko, Y.; Sugihara, H.; Moritomo, H.; Suzuki, Y.; Kawamata, J.; Konishi, G. *J. Mater. Chem. B* **2015**, *3*, 161−162.

(21) Greenspan, P.; Mayer, E. P.; Fowler, S. D. *J. Cell Biol.* **1985**, *100*, 965−973.

(22) Surry, D. S.; Buchwald, S. L. *Chem. Sci.* **2011**, *2*, 27−50.

(23) Astakhova, I. V.; Korshun, V. A.; Wengel, J. *Chem. - Eur. J.* **2008**, *14*, 11010−11026.

(24) Goltz, M.; Murata, I. *Bull. Chem. Soc. Jpn.* **1988**, *61*, 3767−3769.

(25) Minabe, M.; Takeshige, S.; Kimura, T.; Tsubota, M. *Bull. Chem. Soc. Jpn.* **1994**, *67*, 172−179.

(26) Harvey, R. G.; Pataki, J.; Lee, H. *Org. Prep. Proced. Int.* **1984**, *16*, 144−148.

(27) Scott, L. T.; Necula, A. *J. Org. Chem.* **1996**, *61*, 386−388.

(28) Wu, X.-F. *Tetrahedron Lett.* **2012**, *53*, 3397−3399.

(29) Niko, Y.; Sasaki, S.; Kawauchi, S.; Tokumaru, K.; Konishi, G. *Chem. - Asian J.* **2014**, *9*, 1797−1807.

(30) Turro, N. J.; Ramamurthyl, V.; Scaiano, J. C. *Modern Molecular Photochemistry of Organic Molecules*; University Science Books: Sausalito, CA, 2010; p 238, pp 277−287.

(31) (a) Lippert, E. L. *Organic Molecular Photophysics*; Wiley-Interscience: New York, 1975. (b) Mataga, N.; Kubota, T. *Molecular Interactions and Electronic Spectra*; Dekker, M.: New York, 1970.

(32) Kucherak, O. A.; Didier, P.; Mély, Y.; Klymchenko, A. S. *J. Phys. Chem. Lett.* **2010**, *1*, 616−620.

(33) Turro, N. J.; Ramamurthyl, V.; Scaiano, J. C. *Modern Molecular Photochemistry of Organic Molecules*; University Science Books: Sausalito, CA, 2010; pp 303−304.

(34) (a) Cortes, J.; Heitele, H.; Jortner, J. *J. Phys. Chem.* **1994**, *98*, 2527−2536. (b) Marcus, R. A. *J. Phys. Chem.* **1989**, *93*, 3078−3086. (c) Herbich, J.; Kapturkiewicz, A. *J. Am. Chem. Soc.* **1998**, *120*, 1014−1029. (d) Kapturkiewicz, A.; Herbich, J.; Karpiuk, J. *J. Phys. Chem. A* **1997**, *101*, 2332−2344.

(35) (a) Weissleder, R. *Nat. Biotechnol.* **2001**, *19*, 316−317. (b) Pu, Y.; Shi, L.; Pratavieira, S.; Alfano, R. R. *J. Appl. Phys.* **2013**, *114*, 153102.

(36) Reichardt, C. *Chem. Rev.* **1994**, *94*, 231−2358.

(37) Terenziani, F.; Painelli, A.; Katan, C.; Charlot, M.; Blanchard-Desce, M. *J. Am. Chem. Soc.* **2006**, *128*, 15742−15755.

(38) Peng, X.; Yang, Z.; Wang, J.; Fan, J.; He, Y.; Song, F.; Wang, B.; Sun, S.; Qu, J.; Qi, J.; Yan, M. *J. Am. Chem. Soc.* **2011**, *133*, 6626−6635.

(39) Kucherak, O. A.; Oncul, S.; Darwich, Z.; Yushchenko, D. A.; Arntz, Y.; Didier, P.; Mély, Y.; Klymchenko, A. S. *J. Am. Chem. Soc.* **2010**, *132*, 4907−4916.

(40) Blanchard, S. C. *Chem. Soc. Rev.* **2014**, *43*, 1044−1056.

(41) (a) Hou, Y.; Bardo, A. M.; Martinez, C.; Higgins, D. A. *J. Phys. Chem. B* **2000**, *104*, 212−219. (b) Hou, Y.; Higgins, D. A. *J. Phys. Chem. B* **2002**, *106*, 10306−10315.

DOI: 10.1021/acs.joc.5b01987
J. Org. Chem. 2015, 80, 10794−10805